JGR Biogeosciences

RESEARCH ARTICLE
10.1029/2019JG005522

Special Section:
Quantifying Nutrient Budgets for sustainable nutrient management

Key Points:

- Continuous and high temporal resolution of ammonia (NH_3) concentrations were measured using cavity ring-down spectroscopy over a salt marsh
- Average diurnal cycles of NH_3 fluxes were estimated in a coastal ecosystem using a new analytical methodology
- Tidal water level was identified as a key parameter influencing NH_3 emissions in wetlands

Correspondence to:
N. Lichiheb,
nebila.lichiheb@noaa.gov

Citation:
Lichiheb, N., Heuer, M., Hicks, B. B., Saylor, R., Vargas, R., Vázquez-Lule, A., et al. (2021). Atmospheric ammonia measurements over a coastal salt marsh ecosystem along the Mid-Atlantic U.S. *Journal of Geophysical Research: Biogeosciences*, *126*, e2019JG005522. https://doi.org/10.1029/2019JG005522

Received 7 NOV 2019
Accepted 19 APR 2021

Author Contributions:
Conceptualization: Nebila Lichiheb
Data curation: Nebila Lichiheb
Formal analysis: Nebila Lichiheb
Investigation: Nebila Lichiheb
Methodology: Nebila Lichiheb
Project Administration: Nebila Lichiheb
Supervision: Nebila Lichiheb
Validation: Nebila Lichiheb
Visualization: Nebila Lichiheb
Writing – original draft: Nebila Lichiheb
Writing – review & editing: Nebila Lichiheb

Atmospheric Ammonia Measurements Over a Coastal Salt Marsh Ecosystem Along the Mid-Atlantic U.S.

Nebila Lichiheb[1], Mark Heuer[1,2], Bruce B Hicks[3], Rick Saylor[1], Rodrigo Vargas[4], Alma Vázquez-Lule[4], Kari St. Laurent[5], and LaToya Myles[1]

[1]National Oceanic and Atmospheric Administration, Atmospheric Turbulence and Diffusion Division, Oak Ridge, TN, USA, [2]Oak Ridge Associated Universities, Oak Ridge, TN, USA, [3]MetCorps, Norris, TN, USA, [4]Department of Plant & Soil Sciences, University of Delaware, Newark, DE, USA, [5]Delaware Department of Natural Resources and Environmental Control, Delaware National Estuarine Research Reserve, Dover, DE, USA

Abstract Measurements of atmospheric ammonia (NH_3) concentrations and fluxes are limited in coastal regions in the eastern U.S. In this study, continuous and high temporal resolution measurements (5s) of atmospheric NH_3 concentrations were recorded using a cavity ring-down spectrometer in a temperate tidal salt marsh at the St Jones Reserve (Dover, DE). Micrometeorological variables were measured using an eddy covariance system which is part of the AmeriFlux network (US-StJ). Soil, plant, and water chemistry were also analyzed to characterize the sources and sinks of atmospheric NH_3. A new analytical methodology was used to estimate the average ecosystem-scale diurnal cycle of NH_3 fluxes by replicating the characteristics of a chamber experiment. This virtual chamber approach estimates positive surface fluxes in continuing strongly stable conditions when mixing with the air above is minimal. Our findings show that tidal water level may have a significant impact on NH_3 emissions from the marsh. The largest fluxes were observed at low tide when more soil was exposed. While it is expected that NH_3 fluxes will peak when the air temperature maximizes, high tide occurred concurrently with midday peaks in solar irradiance led to a decrease in NH_3 fluxes. Furthermore, soil, plant, and water chemistry measurements underpinning the NH_3 concentrations and fluxes lead us to conclude that this coastal wetland ecosystem can act as either a sink or a source of NH_3. Such measurements provide novel data on which we can base reliable parameterizations to simulate NH_3 emissions from coastal salt marsh ecosystems using surface-atmosphere transfer models.

Plain Language Summary Coastal wetlands such as salt marshes, mangroves, and seagrasses provide a natural environment for the sequestration and long-term storage of carbon dioxide (CO_2) from the atmosphere. As a fertilizer, nitrogen (N) increases the vegetative growth and thus more CO_2 may be fixed in plants as biomass representing the short-term storage pool of carbon, therefore reducing its atmospheric level. Salt marshes, in particular, have been identified as being highly effective at carbon sequestration as well as adsorbing and transforming N. However, there are limited atmospheric measurements of ammonia (NH_3) concentrations and exchanges in coastal areas of the Eastern and Mid-Atlantic U.S. This pilot study represents one of the few atmospheric measurements of NH_3 over temperate tidal salt marshes in the Mid-Atlantic U.S. The high temporal resolution measurements of NH_3 concentrations indicated that local sources, such as agriculture and industry, may have a considerable impact on the local atmospheric NH_3 concentrations. The results also show that tidal water levels in salt marshes may have a significant effect on NH_3 emissions.

1. Introduction

Terrestrial-aquatic interfaces such as salt marshes, mangroves, and similar coastal wetlands occupy only a small fraction of the Earth's surface but account for at least 50% of the total carbon sequestration to ocean ecosystems (Duarte et al., 2005). Carbon sequestered and stored in coastal ecosystems and oceans is known as blue carbon (Mcleod et al., 2011) and there is a need to improve Earth system models across such coastal interfaces (Ward et al., 2020). These ecosystems are carbon-rich and play important roles in greenhouse gas biogeochemistry and the cycling of nutrients, including nitrogen (N) and phosphorus (Mcleod et al., 2011). The rapid loss (1%–3%/yr) of these coastal ecosystems, due to a variety of natural and anthropogenic disturbances, results in substantial impacts on carbon sequestration, carbon storage capacity, and nutrient cycling

(Duarte et al., 2013). The loss rate of these critical ecosystems may accelerate in the future due to changing weather, climate, sea level rise, and land use, as well as high-impact events like hurricanes and wildfires (Kirwan & Megonigal, 2013).

Salt marshes, in particular, have been identified as being highly effective at carbon sequestration and adsorbing and transforming N (Loomis & Craft, 2010; Mcleod et al., 2011; Ouyang & Lee, 2014); however, the loss of these important ecosystems has accelerated in recent decades. One reason for the declining extent of salt marshes worldwide may be related to the increased anthropogenic perturbation of the global biogeochemical cycles of N (Peñuelas et al., 2013). Previous studies have suggested that salt marsh eutrophication can have large negative impacts on the capacities of these ecosystems for climate mitigation (Chmura et al., 2016; Deegan et al., 2012). There are over 4 million acres of salt marsh in the US and over half of these are along the Atlantic coast of the US (Field et al., 1991). These areas experience large rates of N pollution mainly due to agricultural activities (e.g., emissions from livestock waste and fertilized crops) (Boyer et al., 2002).

Ammonia (NH_3) is the most abundant alkaline gas in the atmosphere (Behera et al., 2013). In addition, NH_3 is a major atmospheric acid-neutralizing compound that plays an important role in the formation of aerosols (Finlayson-Pitts & Pitts, 1999; Saylor et al., 2015) which adversely affect human health (Pope & Dockery, 2006), reduce visibility (Battye et al., 2016; Bray et al., 2017), alter Earth's radiative balance, and contribute to reactive nitrogen (Nr) global redistribution through the atmospheric deposition (Galloway et al., 2013; Pinder et al., 2008). Agricultural intensification is the primary anthropogenic source of NH_3 leading to a doubling of Nr entering the biosphere (Galloway et al., 2004). Other sources of NH_3 include industrial processes, vehicular emissions and volatilization from soils and oceans (Behera et al., 2013). Agricultural and urban sources that emit NH_3 directly or indirectly through atmospheric deposition processes (Howarth et al., 1996; Ryan & Boyer, 2012) are known to alter the structure and functions of salt marshes (Geoghegan et al., 2018). Furthermore, atmospheric deposition processes have been identified as the main route of entry for NH_3 into coastal waters (Paerl & Fogel, 1994), and the deposition of NH_3 to sensitive ecosystems (e.g., salt marshes) can lead to a series of negative effects such as soil acidification, eutrophication and loss of biodiversity (Catovsky et al., 2002; Wallace et al., 2014).

Despite this, there are limited atmospheric measurements of NH_3 concentrations and fluxes in coastal areas of the Eastern and Mid-Atlantic U.S (Amos et al., 2018; Larsen et al., 2001; Poor et al., 2001; Siefert et al., 2002). The few experimental studies in the literature used a combination of conventional air sampling techniques such as annular denuders, filter packs, and passive filter badges to calculate the NH_3 concentrations. These techniques are relatively easy to deploy and inexpensive. However, they require long integration times (hours to days of sampling) and are often labor-intensive. Siefert et al. (2002) proposed a measurement technique which provides a higher temporal resolution (10 min) in the measurement of atmospheric NH_3 concentrations by coupling a mist chamber with a fluorometer instrument. This method improved the temporal resolution of NH_3 measurements, but it can only continuously measure NH_3 unattended for a period of two days. In recent years, fast-response techniques, such as cavity ring-down spectroscopy (CRDS), have been successfully deployed to continuously measure atmospheric NH_3 (Nelson et al., 2019; Shadman et al., 2016; von Bobrutzki et al., 2010) and emissions from soils (Petrakis et al., 2017) and tree stems (Barba et al., 2019). This new technology provides improved temporal resolution of NH_3 measurements, which is necessary given the dynamic response of NH_3 to changing environmental conditions (Kamp et al., 2019). Continuous and high temporal resolution measurements of atmospheric NH_3 concentrations in salt marsh ecosystems along the east coast of the US are needed to provide details of the fluctuations of NH_3 concentrations (Amos et al., 2018). Such detailed measurements will make it possible to accurately calculate the NH_3 flux between the atmosphere and the surface in salt marshes.

Deep sediments in salt marshes create anaerobic environments where many of the plants, such as *Spartina alterniflora,* are adapted to the daily flooding, variations in salinity, and periodic low O_2 in the root zone (Seyfferth et al., 2020). Under these anaerobic conditions the microbial community plays an important role in regulating production and emission of NH_3 from wetlands (Inglett et al., 2005). The question of whether salt marshes act as sinks of atmospheric NH_3 or as sources of it remains to be addressed, and to this end, measurements of the fluxes of NH_3 are required.

There are even fewer measurements of NH_3 fluxes over the salt marsh ecosystem. In most contemporary studies of atmospheric fluxes, eddy covariance (EC) or gradient methods are preferred. The application of these methods involves complex instrumentation and requires site uniformity that is difficult to satisfy in coastal environments. In such circumstances, alternative methods are required to derive information regarding fluxes at the surface of the chemical species of interest, in this case NH_3. The experimental study and analysis described here provides detailed information to enable the estimation of NH_3 fluxes, using a statistical approach in which micrometeorological field data are used to replicate the likely characteristics of a chamber experiment. This new method yields estimates of the average diurnal cycle of NH_3 fluxes over weekly (or longer) periods.

The purpose of this study was to advance our process-level understanding of NH_3 air-surface exchange over a coastal salt marsh ecosystem along the Mid-Atlantic U.S. Here, we present continuous and high temporal resolution measurements of atmospheric NH_3 concentrations in the St Jones Reserve, a component of the Delaware National Estuarine Research Reserve (DNERR). These high temporal resolution measurements allowed the estimation of the average diurnal cycle of NH_3 fluxes using a new analytical methodology. The study site was selected because it has extensive micrometeorological instrumentation and information about trace gas dynamics as part of the US AmeriFlux network. Furthermore, soil, plant, and water chemistry were analyzed to characterize the sources and sinks of atmospheric NH_3 in this ecosystem. A central goal was to identify and quantify the key parameters influencing NH_3 emissions in wetlands, such as tidal water level.

2. Materials and Methods

2.1. Site Description and Meteorological Measurements

The field study took place at the St. Jones Reserve (39° 5′17.53″N 75°26′13.77″W, 6.7 m average elevation above sea level) from June 21 to July 20, 2018. It is situated along a mesohaline tidal tributary of the St. Jones River located ~6 km upstream of Delaware Bay and at the lower end of the St. Jones River watershed. It is located in southeast Dover, Delaware, USA (Figure 1). The site is located in a tidal marsh influenced by surrounding agricultural fields along the watershed. Dover Air Force Base is nearby and has a considerable presence on the northwestern sides of the St. Jones Reserve. The climate is temperate, with a mean annual temperature of 13.3°C and mean annual precipitation of 1,119 mm. Vegetation at the site is dominated by the saltmarsh cordgrass *Spartina alterniflora* (90%) and is inundated twice a day due to the semi-diurnal tidal cycle. The average plant height of *Spartina alterniflora* recorded during the field experiment was 65.5 ± 8.0 cm with a mean leaf area index of 2.65 ± 0.21. The tidal marsh platform at the St. Jones Reserve is regularly inundated by tidal waters, which range widely in salinity from 0.1 to 29.9 psu (mean 11.2 psu) depending on tidal cycle, season, and precipitation events. The marsh soils are classified as a silty clay loam containing 10% sand, 61% silt, and 29% clay (Capooci et al., 2019).

Instruments were deployed over the marsh from the edge of a small wooden boardwalk (1.7 m width) adjacent to an existing AmeriFlux site (US-StJ) hosted by the University of Delaware (Trifunovic et al., 2020). AmeriFlux is a network of sites that measure carbon dioxide (CO_2), water, and energy fluxes in different ecosystems across the USA and include sites across the Americas (Hargrove et al., 2003). The St. Jones AmeriFlux site provides measurements of CO_2, methane (CH_4), water vapor, and energy fluxes from an EC tower. Instrumentation was deployed at 3.5 m above the surface (~2.5 m above the vegetative canopy) (Figure 2). The EC tower was equipped with a WindMaster Pro anemometer (Model 160724, Gill Instruments, Lymington, Hamisphere, UK), a closed path CO_2/H_2O Analyzer (Model LI-7200RS, LI-COR Environmental, Lincoln, NE, USA) and an open path CH_4 analyzer (Model LI-7700, LI-COR Environmental, Lincoln, NE, USA).

The EC tower also carried instruments to measure air temperature and relative humidity (Probe HMP155, Vaisala, Helsinki, Finland), net radiation (CNR4 Net Radiometer, Kipp & Zonen B.V., Delft, The Netherlands). Soil temperature and soil moisture were also measured (ML2x Theta Soil Moisture Probe, Delta-T Devices, Cambridge, UK). All of these variables were measured at high temporal frequency (10 Hz). The data collected by this tower system are publicly available from the AmeriFlux Network at http://ameriflux.lbl.gov/sites/siteinfo/US-StJ. In addition, DNERR collects 15 min meteorological data (e.g., precipitation,

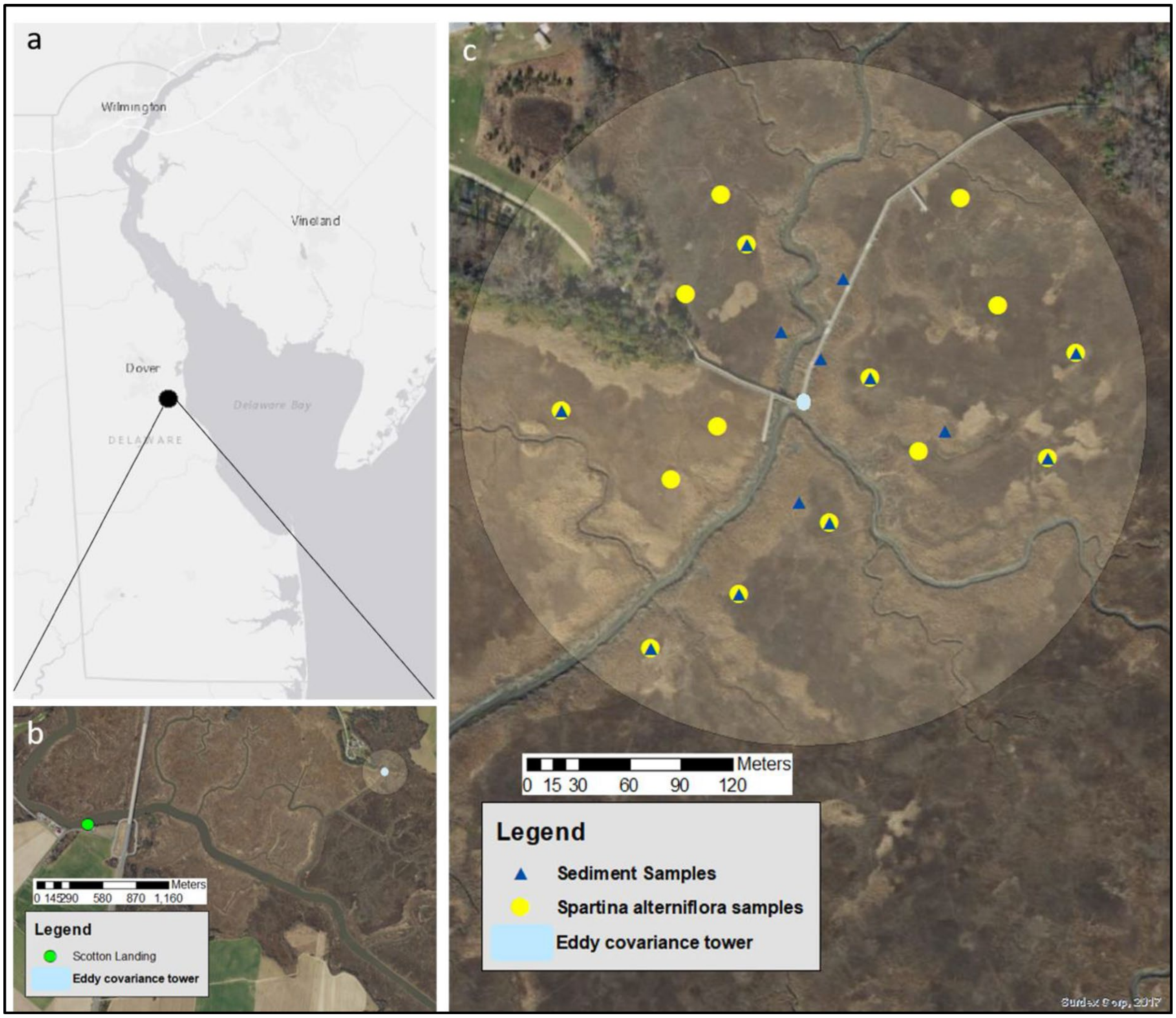

Figure 1. Study site location: (a) geographical context, (b) nutrient data site (Scotton Landing), and (c) sampling zone of plants and sediment within the 200 m radius from the eddy covariance (EC) tower.

air temperature, wind speed and direction, relative humidity) as part of the System-Wide Monitoring Program, using a Campbell Scientific weather station. DNERR meteorological data are available at https://cdmo.baruch.sc.edu/dges/. For this study, DNERR's total precipitation measured with a tipping bucket rain gauge (Model TE 525, Texas Electronics, TX, USA) was used in the analysis.

2.2. Soil, Plant and Water Sampling and Analysis

Plant and soil samples were collected within a 200 m radius from the EC tower (Figure 1). Sample locations were selected using the Random Points tool in ArcGIS (desktop version 10.6). *Spartina alterniflora* was collected on DOY (Day of Year) 180 and 200 by collecting 15 replicates during each sampling with at least 30 g of plant material per sample using a 10 × 10 cm quadrat. Soil was sampled only on DOY 200 by collecting 15 replicates at 0–5 cm of depth with at least 20 g of soil material per sample. Soil and plant samples were analyzed at the Department of Crop and Soil Science of the North Carolina State University.

The National Estuarine Research Reserve System (NERRS), established by partnerships between the National Oceanic and Atmospheric Administration (NOAA) and coastal states in the US, conducts large-scale water quality monitoring for the purposes of increasing understanding of the nation's estuarine waters and contributing to effective coastal zone management. The NERRS System-Wide Monitoring Program tracks

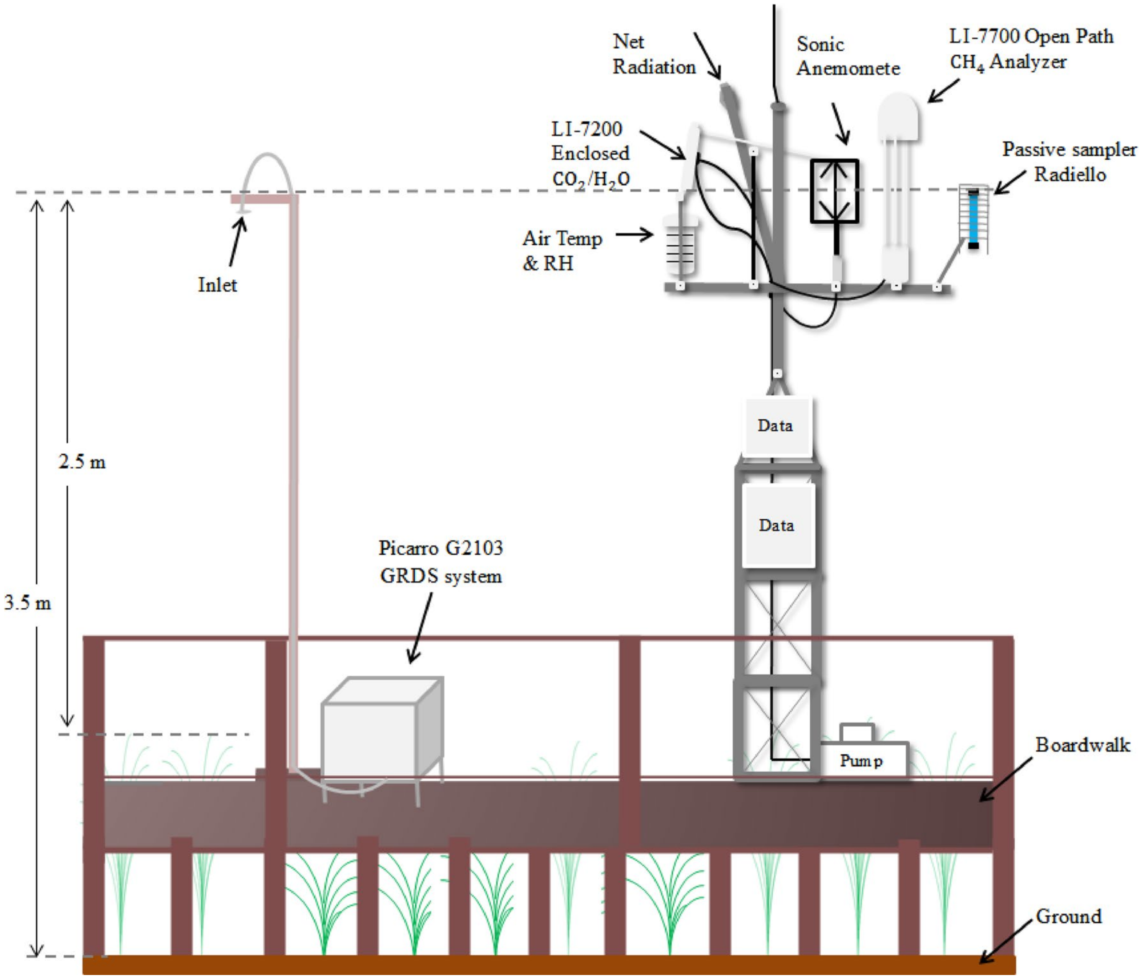

Figure 2. Schematic of the eddy covariance (EC) tower, the passive sampler (Radiello) and the Cavity Ring Down Spectrometer (CRDS).

short-term variability and long-term changes in coastal ecosystems represented by the 29 Reserves within the NERRS. This program has focused primarily on monitoring a suite of physical water quality and atmospheric information since 1996. Water quality measurements using a YSI sonde (current model EXO2 multiparameter sonde) are made every 15 min of water temperature, pH, water level (relative to NAVD88), specific conductivity, salinity, and dissolved oxygen. As part of a recent enhancement to water quality monitoring, the reserve system began monitoring nutrient levels in 2002. The current nutrient monitoring program includes the collection of monthly diel water samples using an Isco 6,700 automatic sampler at one representative station. A total of 11 water samples are collected at 2.5 h intervals over a 25 h period during each sampling event. Water samples are then analyzed for dissolved inorganic N, such as NH_4^+ and NO_3^-. In the present study, we collected water quality and nutrient data from the St. Jones Reserve tidal creek at the Scotton Landing station (39.08498, 75.46058) which is the nearest station from our study site (about 3 km from the EC tower). At this station, water samples were collected on DOY 197. Water temperature, pH and water level data were also collected every 15 min over the study period at the Scotton Landing station.

2.3. NH_3 Concentration Measurements

The concentration of NH_3 was continuously measured using a CRDS instrument (model G2103; Picarro Inc., Santa Clara, CA) every 5s. An enclosure was installed on the outside rim of the boardwalk to install the CRDS. The inlet line of the CRDS was mounted at 3.5 m above the ground (around 2.5 m above the canopy), which was the same measurement height as the EC system (Figure 2). The response time for the whole system was <3 min for a 63% change before and after deployment. The lower detection limit of this instrument for NH_3 is <0.06 μg m^{-3} with an accuracy of (±5% of reading + 0.35 μg m^{-3}) for a 300 s averaging time. CRDS is a laser absorption technique, which measures the lifetime of photons reflected between two mirrors in an optical cavity and determines the sum of sample extinction between the cavity mirrors, enabling quantification of NH_3 concentration by the strength of near-infrared absorption (Scherer et al., 1997). The advantage of this method is that it allows absorption measurements using very long optical path lengths (effective path length up to 20 km) while maintaining a closed optical cell to enable single point measurements (Moosmüller et al., 2005).

The CRDS system was connected to the Picarro system pump sampling at 1 L min^{-1}. The CRDS and pump were housed in an air-conditioned enclosure unit in which the temperature was adjusted to 10°C below ambient to prevent overheating. The CRDS was initially calibrated by the manufacturer. Additionally, the calibration was verified using a short polyvinylidene fluoride vented inlet tube, and zero and span compressed gas cylinders according to manufacturer directions. The zero check was performed with ultrahigh purity N_2 (99.999%) and the span adjustment was performed using 715.8 μgm^{-3} (1,030 ppb ± 5%) NH_3 (NIST-traceable reference gas; Air Liquide: Plumsteadville, PA). The zero and span checks were within the tolerance of the manufacturer's calibration with offset of ~0.8 ppb and span of ~1,135 ppb.

Ambient NH_3 concentration data were also collected using passive samplers (model Radiello®123-7, Supelco: Bellefonte,PA) at the study site. The passive sampler was set up on the EC tower at the same measurement height (2.5 m above the canopy) (Figure 2). Passive samplers were used in accordance with NADP SOP SS-4070 for monitoring ambient NH_3 on a weekly time interval (NADP, 2013).

2.4. Estimation of the Average Diurnal Cycle of NH_3 Fluxes

The analytical method presented by Hicks et al. (2021) and as briefly described below (and appended) has been adapted to derive the average diurnal cycle of NH_3 fluxes by considering the study site as a virtual chamber. Assuming a solid lid across the top of the tidal marsh, extending from edge to edge at height $\boldsymbol{h}$, and if the flux from the surface of NH_3 ($\mathbf{F_{NH_3}}$) was constant, then the concentrations of NH_3 within the confined layer would increase as determined by the wind speed ($\boldsymbol{u}$) and the fetch ($\boldsymbol{x_f}$). Then the concentration in the air ($\mathbf{C_{NH_3}}$) at any distance $\boldsymbol{x_f}$ downwind of the edge will equilibrate as:

$$C_{NH_3} = F_{NH_3} \cdot x_f / \left(h \cdot u\right) \tag{1}$$

This box model approximates the methodology used in chamber studies. In our study, we consider the obvious fact that $\mathbf{F_{NH_3}}$ can be derived as:

$$F_{NH_3} = C_{NH_3} \cdot h \cdot \left(u / x_f\right) \tag{2}$$

The measurements made in this study are used to enable a statistical examination of the marsh and its NH_3 emissions. For any particular measurement, we know the fetch ($\boldsymbol{x_f}$) and the wind speed ($\boldsymbol{u}$). In addition, to put a lid on the conceptual box, we need to consider the case in which there is no turbulent exchange with the air above. In practice, the indicator of transfer through the top of this conceptual chamber is presently taken to be measurement by sonic anemometer of the standard deviation of the vertical wind component (σ_w). The top of the virtual chamber is then defined, as the level of the sonic anemometer.

The following variables can be defined from the available data:

$$X_1 = d\,C_{NH_3} / dt \tag{3}$$

$$X_2 = u / x_f \tag{4}$$

$$X_3 = \sigma_w \tag{5}$$

A multiple regression of X_1 on X_2 and X_3 will yield a relationship of the form:

$$X_1 = a + b_{12} \cdot X_2 + b_{13} \cdot X_3. \tag{6}$$

which is equivalent to:

$$dC_{NH_3} / dt = a + b_{12}\left(u / x_f\right) + b_{13}\sigma_w \tag{7}$$

where b_{12} is the slope between variable 1 and variable 2 and b_{13} is the slope between variable 1 and variable 3. The quantity $\boldsymbol{a}$ represents the rate of change of [NH_3] with time when the defining characteristics of a classical chamber experiment are approached, which are: (i) turbulent diffusion across some specified height can be extrapolated to zero, (ii) wind speed can likewise be extrapolated to zero and (iii) the fetch can be extrapolated to infinity. For our conceptual case, the "box" is lidded by $\sigma_w = 0$.

The quantity $\boldsymbol{a}$ is derived from the analysis requirement that the plane defined by the results must pass through the average of $X_{1,}$ X_2 and X_3.

Hence

$$a = X_1 - b_{12} \cdot X_2 - b_{13} \cdot X_3 \tag{8}$$

The intercept $\boldsymbol{a}$ is then the statistical quantification of the rate of change in concentration that would have been found if a physical chamber were actually present, of height 3.5 m (the height of the EC tower in this case). Then F_{NH_3} (i.e., flux of NH_3) from the surface is then:

$$F_{NH_3} = 3.5 \cdot a \tag{9}$$

The underlying concept is that when NH_3 is emitted from the surface, and if its transfer with the air above is constrained, then the concentrations in the layer in contact with the surface must increase. This requires that there be minimal mixing with air above, and hence the requirement that vertical mixing is minimal is introduced here through the use of σ_w as a key factor. Reliance on u/fetch as a second requirement is so that the situation being addressed through the use of the statistics can lead to a measure of the limit as the wind speed drops to zero (i.e., as advection is eliminated) and as the fetch trends to infinity. This heuristic view of the experimental circumstance is only partially satisfying, because a limitation is introduced through the assumption that dC/dt measured at some specific height relates proportionally to the surface flux once the depth of the affected layer of air is specified. In simple terms, the present approach assumes that gas concentrations are constant with height within the affected layer.

3. Results and Discussion

3.1. N in Soil, Plant and Water

In general, tidal marsh vegetation begins to grow in the spring, reaches peak biomass in the summer, and enters senescence in the fall (Cahoon et al., 2006) depending on factors such as temperature and precipitation. Based operationally on past vegetation surveys conducted at the DNERR, peak biomass occurs between Mid-July through Mid-August. A PhenoCam affixed to the EC tower shows that tidal marsh vegetation in 2018 began to grow at the end of April and reached a peak around Mid-July (Trifunovic et al., 2020).

During this observation period, fresh plant tissue was analyzed at the beginning (DOY 180) and at the end (DOY 200) of the experiment (Table 1). The total N and the fresh plant tissue NH_4^+ concentration decreased over time for *Spartina alterniflora*, while the pH remained almost constant with an average of 6.04 ± 0.14. The decrease in total N and fresh plant tissue NH_4^+ concentrations is related to the growth stages of the plant. In fact, vegetation nutrient concentrations for wetland plants tend to be highest early in the growing season, decreasing as the plant matures and senesces (Bernard & Hankinson, 1979). The range of measured fresh plant tissue NH_4^+ concentration from this study (416.53–763.47 mg kg^{-1}) is much higher than the fresh plant tissue NH_4^+ concentration (31 ± 16 mg kg^{-1}) measured from sunlit vegetation (mix of wax myrtle, leatherwood and inkberry) at the Pocosin Lakes National Wildlife Refuge on the coastal plain of North Carolina (Walker et al., 2014). Differences between our results and those of Walker et al. (2014) may be related to various factors, such as plant species and extraction techniques. Mean NH_4^+ concentration from

Table 1
Mean and Standard Deviation (±) of Total N, NH_4^+ and (NO_3^-) Concentrations, Along With pH From Plant, Soil and Water Sampled During the Experimental Study

Sampling day		Plant	Soil	Water
DOY 180	Total N (mg kg^{-1})	9,833.33 ± 1,237.89	-	-
	NH_4^+ (mg kg^{-1})	763.47 ± 351.59	-	-
	pH	6.09 ± 0.15	-	-
DOY 197	NH_4^+ (mg L^{-1})	-	-	0.07 ± 0.02
	NO_3^- (mg L^{-1})	-	-	0.08 ± 0.02
	pH	-	-	7.40 ± 0.32
DOY 200	Total N (mg kg^{-1})	7,066.67 ± 1,272.04	6,425.0 ± 2,194.39	-
	NH_4^+ (mg kg^{-1})	416.53 ± 104.36	41.73 ± 18.87	-
	NO_3^- (mg kg^{-1})	-	0.24 ± 0.15	-
	pH	5.99 ± 0.10	6.67 ± 0.32	-

Abbreviations: N, nitrogen; NH_4^+, ammonia; NO_3^-, nitrate.

dry soil at 5 cm depth was 41.73 ± 18.87 mg kg^{-1}. NH_4^+ concentration from dry soil sampled in our study is also higher than the NH_4^+ concentration from dry soil measured at 10 cm depth at the Pocosin ecosystem (10.5 mg kg^{-1}). The NH_4^+ and NO_3^-concentrations in the water were 0.07 ± 0.02 mg L^{-1} and 0.08 ± 0.02 mg L^{-1}, respectively. The sum of NH_4^+ and NO_3^-concentrations (0.12 ± 0.04 mg L^{-1}) from water was close to the mean annual total N concentrations measured in Tampa Bay for the 1980–2013 period (0.2–1.2 mg L^{-1}) (Greening et al., 2014). The soil is slightly acidic with a mean pH of 6.67 ± 0.32 (Table 1), and water pH is slightly alkaline ($pH = 7.40 \pm 0.32$). This result is within the range of measured pH in Delaware estuarine waters for the 2002–2016 period from the Scotton Landing SWMP station (6.8–7.9) (Baumann & Smith, 2018).

3.2. Meteorological Conditions

During the field study the air temperature varied from 13.6°C to 34.0°C with an average of 25.0°C. The wind speed averaged 2.0 m s^{-1} and varied from 0 to 5.7 m s^{-1}. Mean water level was 0.29 m and varied from −0.46 and 1.01 m. The water temperature measured from the St. Jones Reserve tidal creek at the Scotton Landing station varied from 20.3°C to 33.8°C with an average of 26.2°C. The water vapor partial pressure varied from 1.1 to 3.5 kPa with an average of 2.3 kPa (Figure 3). The experimental period was quite dry, with sporadic rain events on June 24 (DOY 175), July 17 (DOY 198) and July 18 (DOY 199) with a maximum of 6.75 mm daily precipitation on July 18 (DOY 199). The accumulated precipitation over the experimental period was 7.05 mm.

3.3. NH_3 Concentrations

Figure 4 shows the atmospheric NH_3 concentrations measured using the CRDS instrument and the Radiello passive sampler at the study site. The concentration of NH_3 was continuously measured using the CRDS instrument during the entire study period. In order to collect more atmospheric measurements of NH_3 the passive sampler was left on site for an additional week because it was set up on the existing EC tower. Therefore, four Radiello passive samplers were deployed, corresponding to four sampling periods: DOY175 to 184, DOY 184 to 192, DOY 192 to 199 and DOY 199 to 207. The continuous NH_3 concentrations from the CRDS are reported as 30 min averages and the passive sampling occurred over a week-long sampling period. The comparison of the mean values of NH_3 concentrations from the CRDS and the Radiello for each of the passive sampling periods indicated that both methods are in good agreement. In fact, NH_3 concentrations measured using the passive sampler over the first, second and third sampling periods were 3.37, 2.68 and 2.81 μg m^{-3}, respectively. In comparison, mean NH_3 concentrations from the CRDS over the first, second and third sampling periods were 3.13 ± 1.66, 1.74 ± 1.17, 2.01 ± 1.29 μg m^{-3}, respectively. Mean

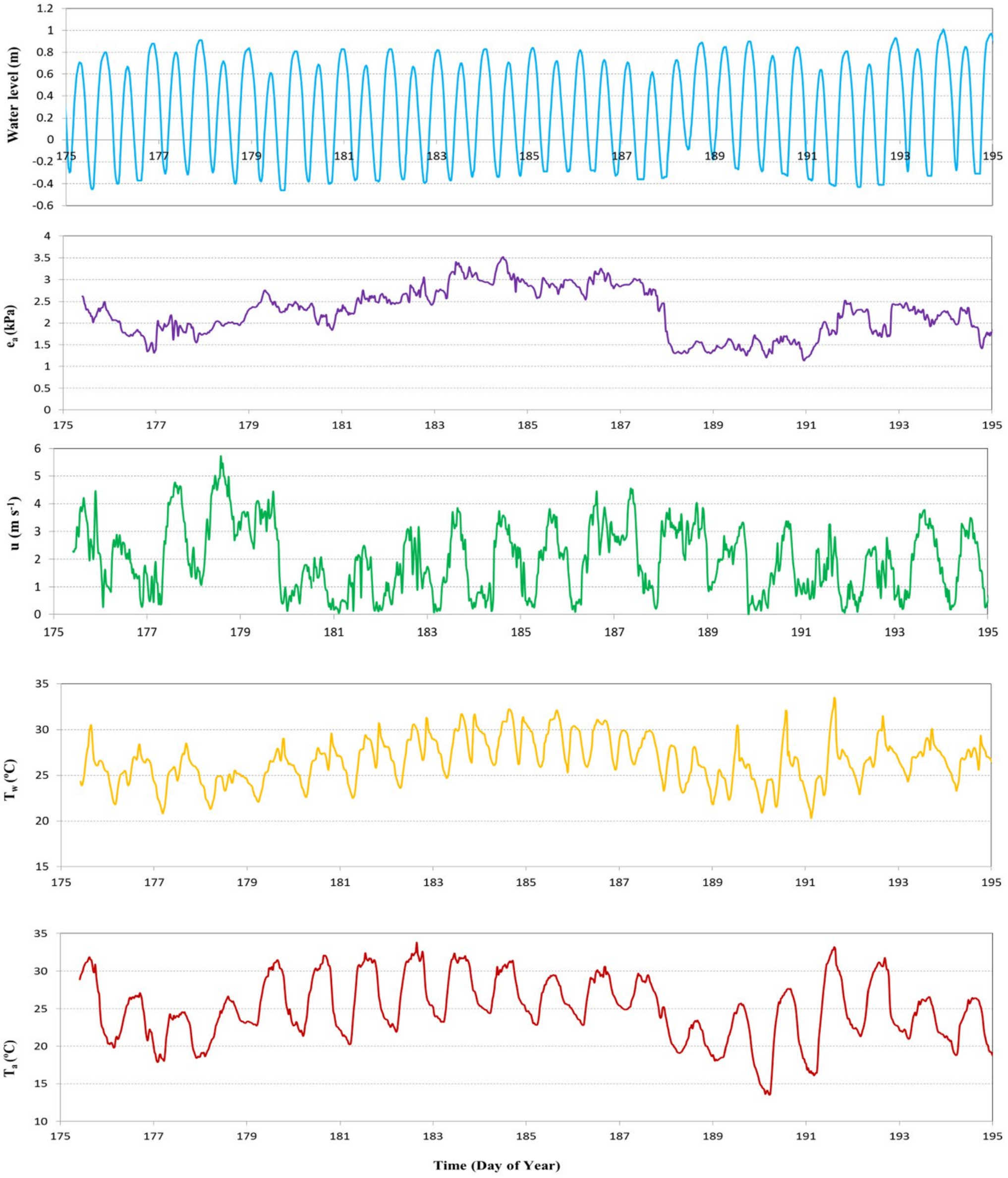

Figure 3. Micrometeorological conditions measured at the site. From top to bottom: water level (NAVD88), vapor pressure (e_a), wind speed (u), water temperature (T_w), and air temperature (T_a).

and standard deviation values of NH_3 concentration from the CRDS and the passive Radiello samplers over the entire experimental study were 2.33 ± 1.53 and 2.95 ± 0.37 μg m^{-3}, respectively. Both methods gave the same range of measured NH_3 concentrations. However, measured NH_3 concentration using the CRDS showed a diurnal pattern with two prominent concentration peaks of 13.25 and 8.82 μg m^{-3} on DOY 175 and 180, respectively. This result illustrates the ability of the CRDS instrument to provide high resolution measurements of atmospheric NH_3 concentrations. This instrument presents a valuable way of improving our process-level understanding of NH_3 emissions in salt marsh ecosystem by providing greater details into the fluctuations of NH_3 concentrations. It should also be noted that the high-resolution measurements provided by the CRDS instrument are particularly challenging in a coastal wetland due to the demanding characteristics of the ecosystem (e.g., high air humidity, salt deposit from the air…). To our knowledge measurements of this kind have not been accomplished previously. The few experimental studies in the literature which measured atmospheric NH_3 in coastal areas generally use a combination of conventional air

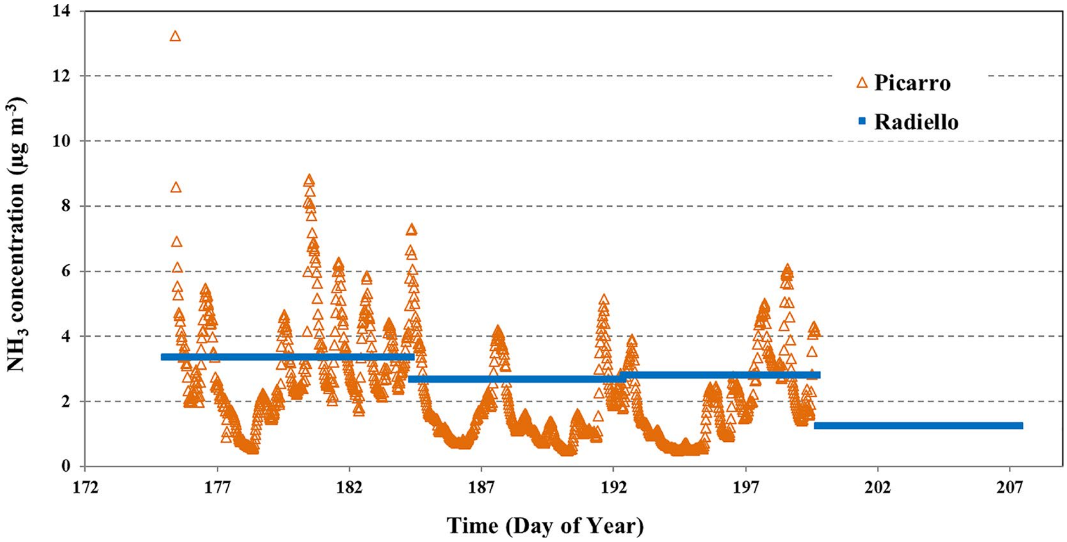

Figure 4. NH$_3$ concentrations as measured using the cavity ring-down spectroscopy (CRDS) and the passive Radiello samplers at the St Jones reserve site. Passive sampling occurred over a one-week sampling period.

sampling techniques such as, annual denuders and filter packs. Those techniques require long integration times and cannot provide the continuous record of short-term measurements on which the present analysis relies.

The average NH$_3$ concentration measured with both methods in this study is in agreement with the total ammonia (NH$_3$ and aerosol ammonium (NH$_4^+$)) concentration measured by Siefert et al. (2002) by coupling a mist chamber to a fluorometer instrument in the Chesapeake Bay during the summer (total NH$_3$ ranged from 0.5 to 7 µg m^{-3}). Larsen et al. (2001) have also measured total NH$_3$ concentrations in the Chesapeake Bay during the summer months using filter packs and denuder systems. The experimental site was located in rural Solomons, close to the Chesapeake Biological Laboratory research pier. The authors reported mean atmospheric concentrations of total NH$_3$ of 1.0 ± 0.8 µg m^{-3}. The NH$_3$ concentration values now reported exceed those found in the Solomons study. Other than differences in biological species, exposed surface area and tidal influences, the difference in measured average NH$_3$ concentrations could result from differences in sampling procedures.

To further investigate the continuous measurements of NH$_3$ concentrations using the CRDS, visual inspection of a wind rose plot was used to study the impact of the surrounding NH3 sources on the local atmospheric NH3 concentration in this natural ecosystem. Figure 5 presents NH$_3$ concentration measured during the entire study period as a function of average wind direction (θ) and mean wind speed (u) reported as 30 min averages. The wind rose shows high NH$_3$ concentrations in most directions, mainly due to the fact that the St. Jones river watershed is dominated by agriculture (38% of the land cover) (Rogerson et al., 2010). The closest farming lands to the present study site are located on the north, northeast and east directions (Rogerson et al., 2010), which explains the high NH$_3$ concentrations (up to 8.82 µg m^{-3}) when winds were blowing from agricultural fields ($5° < \theta < 121°$). This result is in agreement with the experimental studies of Siefert et al. (2002) and Larsen et al. (2001), indicating that high NH$_3$ concentrations in the coastal atmosphere may occur when winds were from agricultural sources due to increased fertilizer usage during the spring and summer and/or due to livestock production. Figure 5 also shows high NH$_3$ concentrations (up to 13.25 µg m^{-3}) when winds were from the wetlands ($152° < \theta < 275°$) located on the west and south directions. This may be related to the microbial activity in anaerobic soils in wetlands which generate NH$_3$ by nitrate reduction pathways (Inglett et al., 2005). The denitrification is the process whereby nitrate is reduced by facultative anaerobic bacteria to nitrous oxides or dinitrogen gas (Johnston, 1991). Poach et al. (2004) demonstrated that NH$_3$ volatilization may be a dominant N removal mechanism by wetlands with 54%–79% of the total N removed. Dover Air Force Base and associated air traffic, which is located within 3 km to the northwestern sides of the St. Jones Reserve, may also have a significant effect on the NH$_3$ concentration when winds were blowing from that direction and even with a wind speed lower than 2 m s^{-1}.

Figure 5. Wind rose derived from the data collected during the entire study period. Red wedges correspond to mean ammonia (NH_3) concentration ($\mu g\ m^{-3}$) as a function of wind direction, and blue wedges correspond to mean wind speed ($m\ s^{-1}$) as a function of wind direction. The background image is a satellite view of the study site location and neighboring areas derived from Google Maps.

Figure 6 shows the average diurnal cycle of NH_3 concentrations, Δe, water level and ΔT during our experiment. As expected, NH_3 concentration (Figure 6a) increases after sunrise, peaks when the air temperature maximizes (between noon and 3 p.m.), and decreases through the following period until the next sunrise. It should also be noted that the water vapor in the air follows the same trend as NH_3 concentration (Figure 6b). This result is considered to indicate that the source area of the NH_3 measured was similar to that of the water vapor, since the water content of the air increased as air moved across the surface, confirming that the NH_3 concentration measurements came from the marsh surface of our study site. The average diurnal cycle of water level (Figure 6c) shows two high tides, a high tide recorded in day time between 8 a.m. and 1 p.m. and the second high tide occurred at night between 8 p.m. and 1 a.m. It can be observed that NH_3 concentration peaks coincide with the midday low tide event occurring between 1:30 and 5:30 p.m. The difference in temperature (ΔT) between the surface temperature, which is the water temperature measured from the St. Jones Reserve Scotton Landing water quality station (about 3 km from the EC tower), and the air temperature was negative in daytime and positive at night (Figure 6d). This result indicates that the situation for the St. Jones Reserve is reversed from what is expected from a land surface, because if the surface were extensive solid land, ΔT would be strongly positive in daytime and negative at night (Oke, 1987). The reverse situation observed at the St. Jones Reserve could be explained by the fact that surface temperatures over water are less extreme than surface temperature over land, because water heats and cools more slowly than land due to the high heat capacity of water. This phenomenon was demonstrated in lake ecosystems by

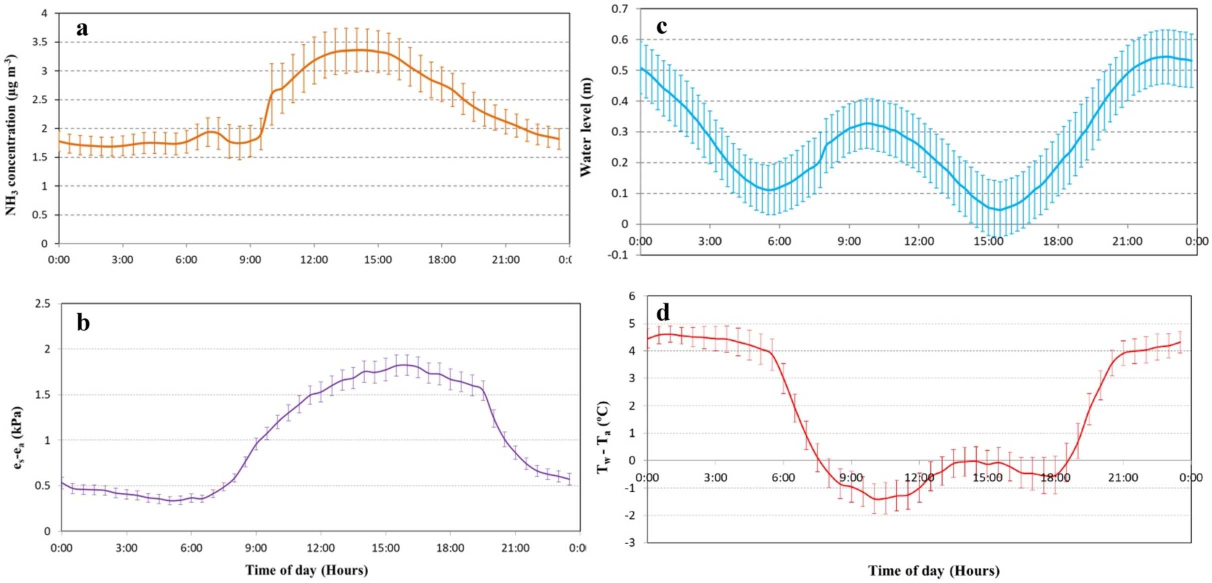

Figure 6. Average hourly diurnal cycle of NH_3 concentrations (a), Δe ($\Delta e = e_s – e_a$) (b), water level (c) and ΔT ($\Delta T = T_w – T_a$) (d). e_s, e_a, T_w and T_a refer to saturated vapor pressure, vapor pressure, water temperature and air temperature respectively. Error bars represent ±1 standard deviation of the mean.

Woolway et al. (2017), who showed evidence of the variations in the stability of the atmospheric boundary layer over lakes and their influence on water and energy exchanges at the air-surface interface. For the present study site, it is clear that the stability regime is reversed from land-based expectations: the surface air is stratified in daytime and unstable at night. As previously explained, the virtual chamber method works best in stable conditions.

3.4. Average Diurnal Cycle of NH_3 Flux Estimation

The concept forming the basis for the calculations made here is based on three key assumptions: (i) NH_3 concentrations are constant with height within the affected layer, (ii) wind speed can be extrapolated to zero and (iii) the fetch can be extrapolated to infinity. Moreover, the virtual chamber methodology necessarily addresses the case of positive surface fluxes in continuing strongly stable conditions. The time sequence of observations shows that the stability is strongest during the daytime, in complete contrast to the situation over land without the presence of the marsh's water and its thermal inertia. Results from the temperature difference between the surface and the air $T_w – T_a$ (Figure 6d) shows that the air in contact with the marsh surface is sometimes stratified at night and frequently stratified in daytime. The central need is to derive an estimate of the surface flux when the air is constrained so that emissions accumulate.

We are interested only in those data for which there is a measured increase in concentrations with time. The data set used in the following has been extracted accordingly, which represent 42.8% of the overall data. In addition, incomplete data sets have been excluded. The remaining data were then ordered according to time of day, and sequential ensembles containing 25 sets of measurements were constructed. Within each ensemble, calculations were made of the averages of each of the key variables, X_1, X_2 and X_3, as above, and also of the products $X_1 \cdot X_2$, $X_2 \cdot X_3$ and $X_3 \cdot X_1$. Standard deviations were also computed: $\sigma(X_1)$, $\sigma(X_2)$ and $\sigma(X_3)$. Following convention, correlation coefficients were computed as follows:

$$R_{12} = \left(X_1.X_2 - X_1.X_2\right) / \left(\sigma\left(X_1\right), \sigma\left(X_2\right)\right) \tag{10}$$

where R_{12} is the correlation coefficient between variable 1 and variable 2.

The slopes b_{12} and b_{13} of a planar best fit were then computed as follows:

$$b_{12} = (\sigma\left(X_1\right) / \sigma\left(X_2\right) \cdot \left(R_{12} - R_{23}.R_{13}\right) / \left(1 - R_{23}^{\wedge 2}\right) \tag{11}$$

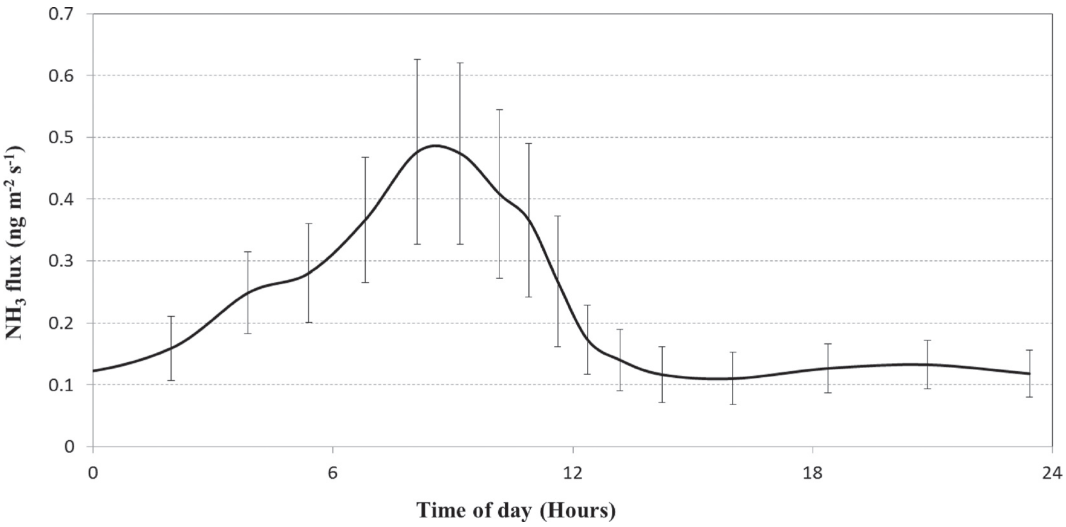

Figure 7. Average diurnal cycle of estimated ammonia (NH_3) fluxes as a function of time. Error bars represent ±1 standard deviation of the mean.

$$b_{13} = (\sigma(X_1) / \sigma(X_3) \cdot (R_{13} - R_{12}.R_{23}) / (1 - R_{23}^{\wedge 2}) \tag{12}$$

where R_{13} is the correlation coefficient between variable 1 and variable 3 and R_{23} is the correlation coefficient between variable 2 and variable 3.

Accordingly, the observations yield a best intercept corresponding to $X_2 = 0$ and $X_3 = 0$ as in Equation 8.

The average diurnal cycle of NH_3 fluxes estimated by the virtual chamber method is presented in Figure 7. The diurnal cycle shows NH_3 emissions gradually increasing from midnight and peaking between 8 and 9 a.m. This peak is followed by a decrease in NH_3 fluxes over time. This early decline in NH_3 fluxes may be attributed to the tidal influences on NH_3 emission in the marsh. Figure 6c shows that during daytime in the study period, the average high tide occurred between 8 a.m. and 1 p.m. Knowing that NH_3 emissions increase exponentially with temperature due to thermodynamic equilibria (Schjoerring, 1997), this high-water level is hypothesized to have led to an abrupt decrease in NH_3 fluxes. To further investigate the role of surface inundation, the NH_3 fluxes were derived as a function of tidal depth. To this end, the data set was ordered according to tidal depth, sequential ensembles of 25 data points were then constructed, and the statistical process outlined above was repeated. The result parallels the diurnal cycle conclusion illustrated in Figure 7, but now indicates the variation according to tidal depth.

Figure 8 shows the average diurnal cycle of NH_3 fluxes as a function of water level. Lower water levels are seen to be associated with high NH_3 fluxes, confirming the plausibility of the suggested mechanism of tidal influences on NH_3 fluxes in this coastal ecosystem. As explained by Vlek and Stumpe (1978), NH_3 volatilization from aqueous systems is directly related to the concentration of ammoniacal N originating principally from the soil. At high tide, only a fraction of the ammoniacal N is retained by the soil and a large fraction is generally found as NH_4^+ in the floodwater. When the water is alkaline (pH above 7.2), ionized NH_4^+ converts to nonionized NH_3 which may escape from the water as a gas. In this context, Vlek and Craswell (1981) reviewed the processes of NH_3 volatilization from flooded soils and concluded that, from a chemical standpoint, NH_3 volatilization is largely determined by the floodwater dynamics, especially NH_4^+ concentration and water pH. In fact, NH_3 volatilization increases with increasing NH_4^+ concentration and water pH. The water analysis results (Table 1) show a water pH of 7.4 and a high NH_4^+ concentration, contributing to nonnegligible NH_3 losses from this natural aquatic ecosystem. Our results are in agreement with several studies carried out to understand the NH_3 volatilization process from rice paddies in order to reduce such losses. Vlek and Craswell (1979) confirmed that NH_4^+ concentration in the rice-paddy floodwater, which is primarily affected by fertilizer application, governs the rate of NH_3 loss from the rice-soil system. In

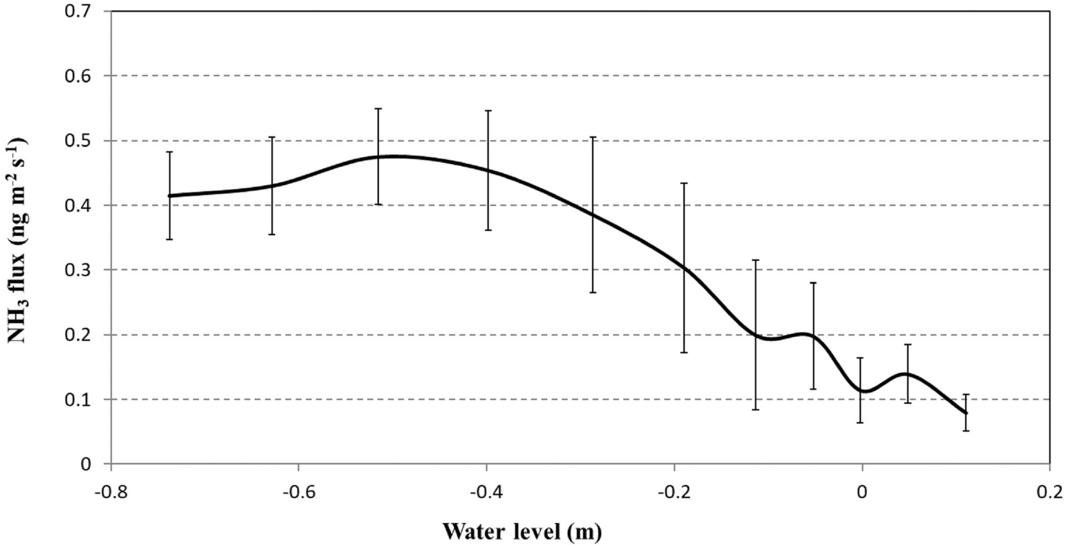

Figure 8. Average NH_3 fluxes as a function of tidal depth. Error bars represent ±1 standard deviation of the mean.

fact, NH_3 volatilization increases with increasing the amount of N fertilizer in flooded rice soil. Mikkelsen et al. (1978) found that the largest NH_3 volatilization rates were registered for a water pH between 7.2 and 10. However, NH_3 losses were negligible from acidic solution (water pH $\leq$ 6.8). In the present study, the atmospheric NH_3 is directly related to the NH_4^+ concentration in the islands. The primary origin of NH_4^+ is linked to the biological activity in the sediments in anaerobic conditions (denitrification process) (McCarthy et al., 1977). In fact, NH_3 fluxes are highest when more soil is exposed as the tidal waters recede (i.e., when the water level is lowest). Furthermore, NH_3 volatilization in aerobic conditions is not considered to be an important mechanism of N loss from flooded soils except where high ammonium concentrations exist in conjunction with high pH of the water (Johnston, 1991). Apart from the chemical factors, NH_3 volatilization in wetlands may be affected by environmental factors, such as temperature and wind speed (Bouwmeester & Vlek, 1981).

4. Conclusions

This research represents the first reported continuous measurements of NH_3 concentrations over a coastal ecosystem using the CRDS technique. Furthermore, it is one of the few atmospheric measurements of NH_3 over a tidal salt marsh in the Mid-Atlantic U.S. The use of the CRDS instrument enabled continuous and high temporal resolution of NH_3 concentrations. This instrument provides greater details of the fluctuation of NH_3 concentrations than standard alternative measurement methods. These high temporal resolution measurements of NH_3 concentrations indicate that local sources, primarily fluxes from the land surface exposed as the tide recedes, have a major influence on NH_3 concentrations measured above the marsh. Distant sources such as agriculture and industry, may also have an impact on the local atmospheric NH_3 concentrations.

Due to site uniformity requirements that are difficult to satisfy in coastal environments, standard EC techniques could not be used to measure NH_3 fluxes at the present location. The matter is explored in more detail in the Appendix, where information from many of the available chemical and meteorological measurement systems is integrated to demonstrate the inapplicability of conventional micrometeorology as a method of relevance here. In the lack of a suitable methodological alternative, a new analytical methodology was used to estimate the average diurnal cycle of NH_3 fluxes. As discussed by Hicks et al. (2021), this method gives an estimate of surface fluxes by replicating the characteristics of a chamber experiment. This virtual chamber methodology is a statistical approach which estimates positive surface fluxes in continuing strongly stable conditions when mixing with the air above is minimal. The average diurnal cycle of NH_3 fluxes estimated by this approach enabled the investigation of the processes influencing NH_3 emissions in wetlands. Our findings show that tidal depth may have a significant effect on NH_3 emissions. In fact, the highest NH_3 fluxes were observed at low tide when more soil/island was exposed. While it is expected that NH_3 fluxes will peak when the air temperature maximizes, high tide occurred concurrently with midday peaks in solar irradiance led to a decrease in NH_3 fluxes.

Soil, plant and water chemistry measurements underpinning the NH_3 concentrations and fluxes provide insights that this salt marsh ecosystem could be either a sink or a source of NH_3. Salt marshes could be a sink of NH_3 via the atmospheric deposition process or a source of NH_3 in anaerobic and aerobic conditions. In anaerobic conditions in deep sediments, the denitrification process is the major pathway of N removal from wetlands. In aerobic conditions, NH_3 volatilization is not considered as an important mechanism of N losses from wetlands except where high NH_4^+ concentrations of the water exist in conjunction with high water pH.

Further measurements of NH_3 concentrations using the CRDS instrument are needed, for longer durations and during different seasons. Moreover, further applications of the new analytical method are also needed because these measurements and estimations may provide data on which we can base reliable parameterizations to simulate NH_3 emissions from coastal salt marsh ecosystems using Surface-Atmosphere transfer models.

Appendix

The St. Jones salt marsh study presents a formidable challenge to experimenters. It is obvious that the water surface imposes a considerable inhomogeneity on the surrounding landscape, and hence determinations of fluxes that can be identified with it impose the need to consider fetch in a more substantial way than is common in conventional micrometeorological studies. In the present case, understanding of the circumstance and their influence on measurements made above the surface is facilitated by the availability of two independent micrometeorological datasets (both based on sonic anemometry) and air concentration data of three trace gases of particular relevance–CO_2, CH_4, and NH_3. The present focus is on NH_3; however, measurements of CO_2 and CH_4, provided for the St. Jones AmeriFlux site (US-StJ) through the AmeriFlux Network at https://ameriflux.lbl.gov/sites/siteinfo/US-StJ#doi, help resolve among the complexities confronting observers.

Figure A1 presents a selection of diagrams to illustrate the difficulties that arise. Plotted in Figure A1 (a) are the average diurnal cycles of the three trace gases of relevance. In each case, concentration measurements C have been normalized to provide comparable indices, $\tilde{C} = (C–\overline{C})/\sigma(C)$, where $\overline{C}$ is the overall average value and σ(C) is the corresponding standard deviation. The diurnal cycles of CO_2 and NH_3 are clearly reversed, with minimum CO_2 concentrations at midday and maximum NH_3. The behavior for CH_4 lies in between. Examination of the stability regimes reveals the reason. Figure A1 (b) shows two measures of atmospheric stability, first the familiar property $\zeta = z/L$. the favored index of micrometeorology derived from eddy flux measurements made well above the surface (q.v. Figure 1). The second stability index is $\xi = (g/\theta)\ (T_w\text{-}T_a)/u^2$, where T_w is water temperature and T_a is air temperature; other notation is conventional. This is an index of stability as it influences the surface itself, whereas ζ represents that stability influencing the air flowing across the surface. The two are not likely to be similar but they display a consistent diurnal cycle, although out of phase. It follows immediately that while measurements of eddy fluxes made above the surface at conventional heights may well be representative of areal averages, the specific role of the water surface now considered is little more than as a small component of the overall areal average that eddy fluxes represent. Relating observed eddy covariances to a specific surface, especially that beneath the location of measurements, is an issue confronting any micrometeorological experiment, leading to considerations of fetch homogeneity, fetch to height ratios, and flux footprints (see Leclerc & Foken, 2014). These familiar deliberations are challenging in the present circumstance, because the turbulence regime below the height of any in-air measurement is not necessarily a sound basis for extending any conventional micrometeorological relationship to the surface itself.

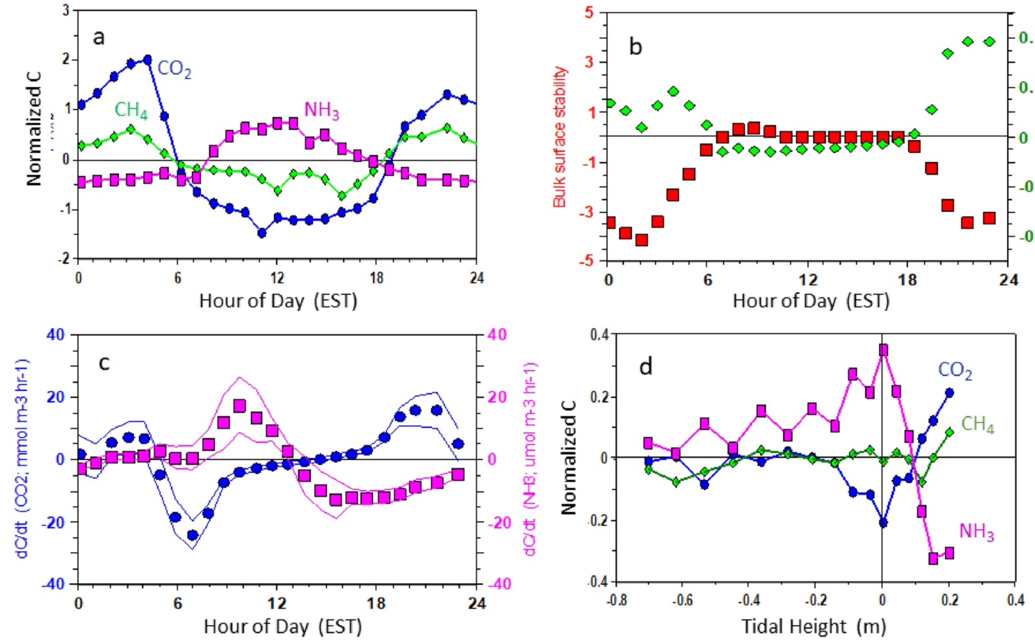

Figure A1. Four examples of indicative characteristics of the association of air above the St. Jones salt marsh with the aquatic surface of the salt marsh. (a) Average normalized concentrations in air (see text) as a function of time of day. (b) The average diurnal cycle of stability, relating to the surface itself and its contact with the air immediately above it (the bulk stability; ξ, in red) and the stability regime of air passing over the surface layer ($\zeta = z/L$, in green). (c) The average diurnal cycles of the rates of change of concentrations of NH_3 (magenta) and CO_2 (in blue). (d) Paralleling (a) but showing the dependence of normalized concentrations on tidal incursion.

The air in contact with the water surface was more often stratified than unstable, as becomes evident when Figure A1 (a) is expanded to show deviations of stability more clearly. In the strong stability regime in the near-surface layer, emissions of a trace gas emitted from the surface will build up as air passes over the surface. In the case of NH_3, such a buildup of concentrations is found to occur most often in the period following dawn, in contrast to convention which decrees that stability regimes are then most quickly becoming unstable. Evidence for this is presented in Figure A1 (c), where the rate of change of NH_3 concentrations in surface air clearly maximizes in the mid-morning, whereas the corresponding CO_2 data indicate that any buildup of CO_2 concentrations during the preceding night is most rapidly depleted in the immediate post-dawn period. Of course, such CO_2 buildup must originate from soil efflux upwind. It cannot be associated with the water surface now considered.

Other considerations arise, regarding the comparative role of NH_3 deposition to the water surface. The exchange of NH_3 between a natural surface and the air is acknowledged to be bidirectional, with the sign of the diffusive exchange being determined by such matters as the pH of the soil and/or water beneath the air layer of interest. In the present case, it is suspected that NH_3 accumulating in the stable surface layer originates from biological activity in the islands that are increasingly exposed as the tidal waters recede. The waters of the salt marsh are intimately exposed to these same sources of NH_3, and it is difficult to imagine a situation in which the fluxes between the water and the air are sufficient to influence the air concentrations as they increase due to the exposed island emissions. Figure A1 (d) substantiates this conclusion. When plotted as a function of water depth, it is seen that average NH_3 concentrations are highest when more soil is exposed (i.e., when the water level is lowest). The evidence is strongest that as solid soil islands first start to be exposed, NH_3 concentrations in air near the surface increase rapidly. At such times, CO_2 (and CH_4) concentrations decrease. But it is not clear that a commonality of cause should be assumed; the situation is complicated by the likely association with CO_2 net ecosystem exchange (and associated CH_4 fluxes) far upwind, beyond the extent of the St. Jones salt marsh. An additional complexity arises from the buoyancy of NH_3. It is lighter than air and hence the analysis considerer here is only relevant to situations in which NH_3 concentrations remain small.

It is not the present purpose to explore the consequences of distant sources and sinks on the CO_2 and CH_4 observations. Instead the analysis presented here is narrowly focused on the NH_3 efflux issue, with methodology developed specifically to derive estimates of the average fluxes from the exposed land surfaces of the salt marsh, given that no conventional flux-gradient methodology is appropriate.

Data Availability Statement

Project data are publicly available for download from NOAA ATDD: https://www.atdd.noaa.gov/denh3.zip.

Acknowledgments
The authors appreciate the support of Kimberly Hutchison from the Environmental and Agricultural Testing Service Laboratory (EATS), Department of Crop and Soil Sciences, at North Carolina State University for analysis of soil and plant samples. The authors gratefully acknowledge the National Atmospheric Deposition Program for providing and analyzing the passive samplers. Much appreciation goes to Dr. Carolyn Currin and her group at NOAA National Centers for Coastal Ocean Science for their scientific advice and support and to D.L. Senn at the NOAA Atmospheric Turbulence and Diffusion Division for dedicated assistance with the field study. The authors also acknowledge the Delaware National Estuarine Research Reserve within the Delaware Department of Natural Resources and Environmental Control for providing very interesting and useful data (https://cdmo.baruch.sc.edu) and hosting this study, particularly NOAA Ernest F. Hollings Scholar Annette Carlson for help with site coordination. R. Varga acknowledges support from the National Science Foundation (grant #1652594).

References

Amos, H. M., Miniat, C. F., Lynch, J., Compton, J., Templer, P. H., Sprague, L. A., et al. (2018). What goes up must come down: Integrating air and water quality monitoring for nutrients. *Environmental Science & Technology*, *52*, 11441–11448. http://doi.org/10.1021/acs.est.8b03504

Barba, J., Poyatos, R., & Vargas, R. (2019). Automated measurements of greenhouse gases fluxes from tree stems and soils: Magnitudes, patterns and drivers. *Scientific Reports*, *9*, 4005. https://doi.org/10.1038/s41598-019-39663-8

Battye, W. H., Bray, C. D., Aneja, V. P., Tong, D., Lee, P., & Tang, Y. (2016). Evaluating ammonia (NH_3) predictions in the NOAA National Air Quality Forecast Capability (NAQFC) using in situ aircraft, ground-level, and satellite measurements from the DISCOVER-AQ Colorado campaign. *Atmospheric Environment*, *140*, 342–351. https://doi.org/10.1016/j.atmosenv.2016.06.021

Baumann, H., & Smith, E. M. (2018). Quantifying metabolically driven pH and oxygen fluctuations in US nearshore habitats at diel to interannual time scales. *Estuaries and Coasts*, *41*, 1102–1117. https://doi.org/10.1007/s12237-017-0321-3

Behera, S. N., Sharma, M., Aneja, V. P., & Balasubramanian, R. (2013). Ammonia in the atmosphere: A review on emission sources, atmospheric chemistry and deposition on terrestrial bodies. *Environmental Science & Pollution Research*, *20*, 8092–8131. https://doi.org/10.1007/s11356-013-2051-9

Bernard, J. M., & Hankinson, G. (1979). Seasonal changes in standing crop, primary production, and nutrient levels in a Carex rostrata Wetland. *Oikos*, *32*, 328–336. https://doi.org/10.2307/3544743

Bouwmeester, R. J. B., & Vlek, P. L. G. (1981). Rate control of ammonia volatilization from rice paddies. *Atmospheric Environment (1967)*, *15*, 131–140. https://doi.org/10.1016/0004-6981(81)90004-4

Boyer, E. W., Goodale, C. L., Jaworski, N. A., & Howarth, R. W. (2002). Anthropogenic nitrogen sources and relationships to riverine nitrogen export in the northeastern U.S.A. *Biogeochemistry*, *57*, 137–169. https://doi.org/10.1007/978-94-017-3405-9_4

Bray, C. D., Battye, W., Aneja, V. P., Tong, D., Lee, P., Tang, Y., & Nowak, J. B. (2017). Evaluating ammonia (NH_3) predictions in the NOAA National Air Quality Forecast Capability (NAQFC) using in-situ aircraft and satellite measurements from the CalNex2010 campaign. *Atmospheric Environment*, *163*, 65–76. https://doi.org/10.1016/j.atmosenv.2017.05.032

Cahoon, D. R., Lynch, J. C., & Hensel, P. F. (2006). Monitoring salt marsh elevation: A protocol for the long-term coastal ecosystem monitoring program at Cape Cod national seashore. *Final protocol to the long-term coastal ecosystem monitoring program*, 104.

Capooci, M., Barba, J., Seyfferth, A. L., & Vargas, R. (2019). Experimental influence of storm-surge salinity on soil greenhouse gas emissions from a tidal salt marsh. *Science of the Total Environment*, *686*, 1164–1172. https://doi.org/10.1016/j.scitotenv.2019.06.032

Catovsky, S., Bradford, M. A., & Hector, A. (2002). Biodiversity and ecosystem productivity: Implications for carbon storage. *Oikos*, *97*, 443–448. https://doi.org/10.1034/j.1600-0706.2002.970315.x

Chmura, G. L., Kellman, L., van Ardenne, L., & Guntenspergen, G. R. (2016). Greenhouse gas fluxes from salt marshes exposed to chronic nutrient enrichment. *PLoS One*, *11*, e0149937. https://doi.org/10.1371/journal.pone.0149937

Deegan, L. A., Johnson, D. S., Warren, R. S., Peterson, B. J., Fleeger, J. W., Fagherazzi, S., & Wollheim, W. M. (2012). Coastal eutrophication as a driver of salt marsh loss. *Nature*, *490*, 388–392. https://doi.org/10.1038/nature11533

Duarte, C. M., Losada, I. J., Hendriks, I. E., Mazarrasa, I., & Marba, N. (2013). The role of coastal plant communities for climate change mitigation and adaptation. *Nature Climate Change*, *3*(11), 961–968.

Duarte, C. M., Middelburg, J. J., & Caraco, N. (2005). Major role of marine vegetation on the oceanic carbon cycle. *Biogeosciences*, *2*, 1–8. https://doi.org/10.5194/bg-2-1-2005

Field, D. W., Reyer, A. J., Genovese, P. V., & Shearer, B. D. (1991). Coastal wetlands of the United States. *National Oceanic and Atmospheric Administration and US Fish and Wildlife Service Washington, DC*, 59.

Finlayson-Pitts, B. J., & Pitts, J. N. (1999). Chemistry of the upper and lower atmosphere: Theory, experiments, and applications. San Diego, CA. Academic Press, 969.

Galloway, J. N., Dentener, F. J., Capone, D. G., Boyer, E. W., Howarth, R. W., Seitzinger, S. P., et al. (2004). Nitrogen cycles: Past, present, and future. *Biogeochemistry*, *70*, 153–226. https://doi.org/10.1007/s10533-004-0370-0

Galloway, J. N., Leach, A. M., Bleeker, A., & Erisman, J. W. (2013). A chronology of human understanding of the nitrogen cycle. *Philosophical Transactions of the Royal Society B: Biological Sciences*, *368*, 20130120. https://doi.org/10.1098/rstb.2013.0120

Geoghegan, E. K., Caplan, J. S., Leech, F. N., Weber, P. E., Bauer, C. E., & Mozdzer, T. J. (2018). Nitrogen enrichment alters carbon fluxes in a New England salt marsh. *Ecosystem Health and Sustainability*, *4*, 277–287. https://doi.org/10.1080/20964129.2018.1532772

Greening, H., Janicki, A., Sherwood, E. T., Pribble, R., & Johansson, J. O. R. (2014). Ecosystem responses to long-term nutrient management in an urban estuary: Tampa Bay, Florida, USA. *Estuarine, Coastal and Shelf Science*, *151*, A1–A16. https://doi.org/10.1016/j.ecss.2014.10.003

Hargrove, W. W., Hoffman, F. M., & Law, B. E. (2003). New analysis reveals representativeness of the AmeriFlux network. *Eos, Transactions American Geophysical Union*, *84*, 529–535. https://doi.org/10.1029/2003eo480001

Hicks, B. B., Lichiheb, L., O'Dell, D. L., Oetting, J., Eash, N. S., Heuer, M., & Myles, L. (2021). A statistical approach to surface renewal: The virtual chamber concept. *Agrosystems, Geosciences & Environment*, *4*, e20141. https://doi.org/10.1002/agg2.20141

Howarth, R. W., Billen, G., Swaney, D., Townsend, A., Jaworski, N., Lajtha, K., et al. (1996). Regional nitrogen budgets and riverine N & P fluxes for the drainages to the North Atlantic Ocean: Natural and human influences. *Biogeochemistry*, *35*, 75–139. https://doi.org/10.1007/bf02179825

Inglett, P. W., Reddy, K. R., & Corstanje, R. (2005). Anaerobic soils. In D. Hillel (Ed.), *Encyclopaedia of soils in the environment* (pp. 72–78). Elsevier Ltd. ISBN: 978-0-12-348530-4. https://doi.org/10.1016/b0-12-348530-4/00178-8

Johnston, C. A. (1991). Sediment and nutrient retention by freshwater wetlands: Effects on surface water quality. *Critical Reviews in Environmental Control*, *21*, 491–565. https://doi.org/10.1080/10643389109388425

Kamp, J. N., Chowdhury, A., Adamsen, A. P. S., & Feilberg, A. (2019). Negligible influence of livestock contaminants and sampling system on ammonia measurements with cavity ring-down spectroscopy. *Atmospheric Measurement Techniques*, *12*, 2837–2850. https://doi.org/10.5194/amt-12-2837-2019

Kirwan, M. L., & Megonigal, J. P. (2013). Tidal wetland stability in the face of human impacts and sea-level rise. *Nature*, *504*, 53–60. https://doi.org/10.1038/nature12856

Larsen, R. K., Steinbacher, J. C., & Baker, J. E. (2001). Ammonia exchange between the atmosphere and the surface waters at two locations in the Chesapeake Bay. *Environmental Science and Technology*, *35*, 4731–4738. https://doi.org/10.1021/es010755l

Leclerc, M. Y., & Foken, T. (2014). *Footprints in micrometeorology and ecology*. Heidelber. Springer. 239. https://doi.org/10.1007/978-3-642-54545-0

Loomis, M. J., & Craft, C. B. (2010). Carbon sequestration and nutrient (nitrogen, phosphorus) accumulation in river-dominated tidal marshes, Georgia, USA. *Soil Science Society of America Journal*, *74*, 1028–1036. https://doi.org/10.2136/sssaj2009.0171

McCarthy, J. J., Taylor, W. R., Taft, J. L., & Jay, L. (1977). Nitrogenous nutrition of the plankton in the Chesapeake Bay. 1. Nutrient availability and phytoplankton preferences. *Limnology & Oceanography*, *22*, 996–1011. https://doi.org/10.4319/lo.1977.22.6.0996

Mcleod, E., Chmura, G. L., Bouillon, S., Salm, R., Björk, M., Duarte, C. M., et al. (2011). A blueprint for blue carbon: Toward an improved understanding of the role of vegetated coastal habitats in sequestering CO_2. *Frontiers in Ecology and the Environment*, *9*, 552–560. https://doi.org/10.1890/110004

Mikkelsen, D. S., De Datta, S. K., & Obcemea, W. N. (1978). Ammonia volatilization losses from flooded rice soils. *Soil Science Society of America Journal*, *42*, 725–730. https://doi.org/10.2136/sssaj1978.03615995004200050014x

Moosmüller, H., Varma, R., & Arnott, W. P. (2005). Cavity ring-down and cavity-enhanced detection techniques for the measurement of aerosol extinction. *Aerosol Science and Technology*, *39*, 30–39. https://doi.org/10.1080/027868290903880

NADP. (2013). *Standard Operating Procedure for Ambient Ammonia Using Radiello-Type Passive Samplers*. SOP Number SS-4070, Revision 5.1.

Nelson, A. J., Lichiheb, N., Koloutsou-Vakakis, S., Rood, M. J., Heuer, M., Myles, L., et al. (2019). Ammonia flux measurements above a corn canopy using relaxed eddy accumulation and a flux gradient system. *Agricultural and Forest Meteorology*, *264*, 104–113. https://doi.org/10.1016/j.agrformet.2018.10.003

Oke, T. R. (1987). *Boundary layer climates* (second edition). London. Methuen. 435.

Ouyang, X., & Lee, S. Y. (2014). Updated estimates of carbon accumulation rates in coastal marsh sediments. *Biogeosciences*, *11*, 5057–5071. https://doi.org/10.5194/bg-11-5057-2014

Paerl, H. W., & Fogel, M. L. (1994). Isotopic characterization of atmospheric nitrogen inputs as sources of enhanced primary production in coastal Atlantic Ocean waters. *Marine Biology*, *119*, 635–645. https://doi.org/10.1007/bf00354328

Peñuelas, J., Poulter, B., Sardans, J., Ciais, P., van der Velde, M., Bopp, L., et al. (2013). Human-induced nitrogen-phosphorus imbalances alter natural and managed ecosystems across the globe. *Nature Communications*, *4*, 2934. https://doi.org/10.1038/ncomms3934

Petrakis, S., Seyfferth, A., Kan, J., Inamdar, S., & Vargas, R. (2017). Influence of experimental extreme water pulses on greenhouse gas emissions from soils. *Biogeochemistry*, *133*, 147–164. https://doi.org/10.1007/s10533-017-0320-2

Pinder, R. W., Gilliland, A. B., & Dennis, R. L. (2008). Environmental impact of atmospheric NH_3 emissions under present and future conditions in the eastern United States. *Geophysical Research Letters*, *35*, 1–6. https://doi.org/10.1029/2008gl033732

Poach, M. E., Hunt, P. G., Reddy, G. B., Stone, K. C., Matheny, T. A., Johnson, M. H., & Sadler, E. J. (2004). Ammonia volatilization from marsh-pond-marsh constructed wetlands treating swine wastewater. *Journal of Environmental Quality*, *33*, 844–851. https://doi.org/10.2134/jeq2004.0844

Poor, N., Pribble, R., & Greening, H. (2001). Direct wet and dry deposition of ammonia, nitric acid, ammonium and nitrate to the Tampa Bay estuary, FL, USA. *Atmospheric Environment*, *35*, 3947–3955. https://doi.org/10.1016/s1352-2310(01)00180-7

Pope, C. A., & Dockery, D. W. (2006). Health effects of fine particulate air pollution: Lines that connect. *Journal of the Air & Waste Management Association*, *56*, 709–742. https://doi.org/10.1080/10473289.2006.10464485

Rogerson, A. B., Jacobs, A. D., & Howard, A. M. (2010). *Wetland condition of the St. Jones river watershed*. Delaware Department of Natural Resources and Environmental Control, Watershed Assessment Section, Dover, USA. 66p.

Ryan, A. B., & Boyer, K. E. (2012). Nitrogen further promotes a dominant salt marsh plant in an increasingly saline environment. *Journal of Plant Ecology*, *5*, 429–441. https://doi.org/10.1093/jpe/rts001

Saylor, R., Myles, L., Sibble, D., Caldwell, J., & Xing, J. (2015). Recent trends in gas-phase ammonia and PM2.5 ammonium in the Southeast United States. *Journal of the Air & Waste Management Association*, *65*, 347–357. https://doi.org/10.1080/10962247.2014.992554

Scherer, J. J., Paul, J. B., O'Keefe, A., & Saykally, R. J. (1997). Cavity ringdown laser absorption spectroscopy: History, development, and application to pulsed molecular beams. *Chemical Reviews*, *97*, 25–52. https://doi.org/10.1021/cr930048d

Schjoerring, J. K. (1997). *Plant-atmosphere ammonia exchange: Quantification, physiology regulation and interaction with environmental factors, D Sc. Thesis, Roy. Veterinary and agric* (p. 55). Danemark. University of Copenhage.

Seyfferth, A. L., Bothfeld, F., Vargas, R., Stuckey, J. W., Wang, J., Kearns, K., et al. (2020). Spatial and temporal heterogeneity of geochemical controls on carbon cycling in a tidal salt marsh. *Geochimica et Cosmochimica Acta*, *282*, 1–18. https://doi.org/10.1016/j.gca.2020.05.013

Shadman, S., Rose, C., & Yalin, A. P. (2016). Open-path cavity ring-down spectroscopy sensor for atmospheric ammonia. *Applied Physics B*, *122*, 1–9. https://doi.org/10.1007/s00340-016-6461-5

Siefert, R. L., Baker, J. E., & Zander, A. K. (2002). *Development and application of a rapid and robust sensor to determine nitrogen species in the coastal atmosphere: A final report submitted to the NOAA/UNH Cooperative Institute for Coastal and Estuarine Environmental Technology (CICEET)*, University of Maryland Center for Environmental Science, Chesapeake Biological Laboratory.

Trifunovic, B., Vázquez-Lule, A., Capooci, M., Seyfferth, A. L., Moffat, C., & Vargas, R. (2020). Carbon dioxide and methane emissions from temperate salt marsh tidal creek. *Journal of Geophysical Research: Biogeosciences*, *125*, e2019JG005558. https://doi.org/10.1029/2019jg005558

Vlek, P. L. G., & Craswell, E. T. (1979). Effect of nitrogen source and management on ammonia volatilization losses from flooded rice-soil systems. *Soil Science Society of America Journal*, *43*, 352–358. https://doi.org/10.2136/sssaj1979.03615995004300020023x

Vlek, P. L. G., & Craswell, E. T. (1981). Ammonia volatilization from flooded soils. *Fertilizer Research*, *2*, 227–245. https://doi.org/10.1007/bf01050196

Vlek, P. L. G., & Stumpe, J. M. (1978). Effects of solution chemistry and environmental conditions on ammonia volatilization losses from aqueous systems. *Soil Science Society of America Journal*, *42*, 416–421. https://doi.org/10.2136/sssaj1978.03615995004200030008x

von Bobrutzki, K., Braban, C. F., Famulari, D., Jones, S. K., Blackall, T., Smith, T. E. L., et al. (2010). Field inter-comparison of eleven atmospheric ammonia measurement techniques. *Atmospheric Measurement Techniques*, *3*, 91–112. https://doi.org/10.5194/amt-3-91-2010

Walker, J. T., Robarge, W. P., & Austin, R. (2014). Modeling of ammonia dry deposition to a pocosin landscape downwind of a large poultry facility. *Agriculture, Ecosystems & Environment*, *185*, 161–175. https://doi.org/10.1016/j.agee.2013.10.029

Wallace, R. B., Baumann, H., Grear, J. S., Aller, R. C., & Gobler, C. J. (2014). Coastal ocean acidification: The other eutrophication problem. *Estuarine, Coastal and Shelf Science*, *148*, 1–13. https://doi.org/10.1016/j.ecss.2014.05.027

Ward, N. D., Megonigal, J. P., Bond-Lamberty, B., Bailey, V. L., Butman, D., Canuel, E. A., et al. (2020). Representing the function and sensitivity of coastal interfaces in Earth system models. *Nature Communications*, *11*, 1–14. https://doi.org/10.1038/s41467-020-16236-2

Woolway, R. I., Verburg, P., Merchant, C. J., Lenters, J. D., Hamilton, D. P., Brookes, J., et al. (2017). Latitude and lake size are important predictors of over-lake atmospheric stability. *Geophysical Research Letters*, *44*, 8875–8883. https://doi.org/10.1002/2017gl073941